

Intraguild predation enables coexistence of competing phytoplankton in a well-mixed water column

HOLLY V. MOELLER,^{1,2,3,4} MICHAEL G. NEUBERT,¹ AND MATTHEW D. JOHNSON¹

¹Biology Department, Woods Hole Oceanographic Institution, Woods Hole, Massachusetts 02543 USA

²Biodiversity Research Centre, University of British Columbia, Vancouver, British Columbia V6T 1Z4 Canada

Citation: Moeller, H. V., M. G. Neubert, and M. D. Johnson. 2019. Intraguild predation enables coexistence of competing phytoplankton in a well-mixed water column. *Ecology* 00(00):e02874. 10.1002/ecs.2874

Abstract. Resource competition theory predicts that when two species compete for a single, finite resource, the better competitor should exclude the other. However, in some cases, weaker competitors can persist through intraguild predation, that is, by eating their stronger competitor. Mixotrophs, species that meet their carbon demand by combining photosynthesis and phagotrophic heterotrophy, may function as intraguild predators when they consume the phototrophs with which they compete for light. Thus, theory predicts that mixotrophy may allow for coexistence of two species on a single limiting resource. We tested this prediction by developing a new mathematical model for a unicellular mixotroph and phytoplankton that compete for light, and comparing the model's predictions with a laboratory experimental system. We find that, like other intraguild predators, mixotrophs can persist when an ecosystem is sufficiently productive (i.e., the supply of the limiting resource, light, is relatively high), or when species interactions are strong (i.e., attack rates and conversion efficiencies are high). Both our mathematical and laboratory models show that, depending upon the environment and species traits, a variety of equilibrium outcomes, ranging from competitive exclusion to coexistence, are possible.

Key words: community ecology; competition; *Micromonas commoda*; mixotrophy; model-data comparison; *Ochromonas*.

INTRODUCTION

Competition among species for limited resources plays a fundamental role in structuring ecological communities. All else equal, when two species are limited by the same available resource, the species that can persist at the lowest level of the resource when grown in isolation will competitively displace the weaker competitor (Tilman 1977, 1990). This R^* theory (where R^* is the resource-availability threshold required for a species to persist) predicts that the composition of an ecological community can be understood by identifying the resources that limit each member species. The same theory holds for light limitation in planktonic communities: Huisman and Weissing (1994) derived I_{out}^* , the “critical light intensity” to which phytoplankton monocultures draw down available light in a well-mixed water column. In their analysis, the phytoplankton with the lowest I_{out}^* competitively excludes all other species.

However, the observed diversity of some communities exceeds predictions grounded in resource theory. For

example, Hutchinson's description of the “Paradox of the Plankton” notes the surprising diversity of phytoplankton communities despite the fact that their member species appear to occupy the same resource niche delimited by the availability of light and abiotic resources (Hutchinson 1961). In part, some of this surprisingly high diversity can be explained by a subtler understanding of resource partitioning among taxa (e.g., use of different forms of nitrogen in phytoplankton; Moore et al. 2002) and by non-equilibrium dynamics (as was Hutchinson's original point; see Hutchinson 1941, 1961).

Trophic interactions can also enhance community diversity above resource-based expectations. In addition to keystone predators, which exert top-down control on community composition by feeding on competitively superior community members (Paine 1969), intraguild predators, species that eat their competitors, may also increase community diversity (Polis et al. 1989, Polis and Holt 1992). Specifically, an intraguild predator that is otherwise a weaker competitor may persist in a community by consuming its competitors (Holt and Polis 1997), a mechanism that has been empirically demonstrated in several cases (Diehl and Feissel 2001, Borer et al. 2003, Price and Morin 2004, Wilken et al. 2013).

Intraguild predation is widespread in biological systems, from protists Diehl and Feissel 2001, Morin 1999) to insects (Wissinger and McGrady 1993, Borer et al. 2003)

Manuscript received 20 August 2018; revised 9 July 2019; accepted 15 July 2019. Corresponding Editor: Jef Huisman.

³ Present address: Department of Ecology, Evolution & Marine Biology, University of California, Santa Barbara, Santa Barbara, California 93106 USA.

⁴ E-mail: holly.moeller@lifesci.ucsb.edu

to mammals (Fedriani et al. 2000), and most attention has been focused on taxa that compete for a living prey item as opposed to a common, abiotic resource (Arim and Marquet 2004). In contrast, in planktonic communities, mixotrophy is a common form of intraguild predation by which predators and their prey compete for an abiotic resource (Thingstad et al. 1996, Wilken et al. 2014b). Mixotrophic species, which combine photosynthesis with phagotrophic heterotrophy, come in two forms: (1) Algae that ingest prey are termed *constitutive mixotrophs* because they maintain and regulate their own permanently incorporated plastids. (2) Protozoa that host symbiotic algae or steal their plastids are known as *non-constitutive mixotrophs* because, in the absence of prey, they lack photosynthetic machinery (Flynn and Hansen 2013, Mitra et al. 2016). Constitutive mixotrophs (referred to as “mixotrophs” hereafter) function as intraguild predators when their prey are the phytoplankton with which they compete for light and inorganic nutrients. Mixotrophs are thought to gain a competitive advantage over phytoplankton because they can continue to obtain limiting nutrients, in addition to organic carbon, by grazing (Rothhaupt 1996b, Mitra et al. 2016). Their ability to supplement their energetic and carbon needs through photosynthesis also gives them a competitive advantage over pure heterotrophs when prey are scarce (Rothhaupt 1996a, Tittel et al. 2003).

To date, most studies of mixotroph persistence have focused on competition for nutrients. A number of theoretical studies have modeled mixotroph persistence in communities that also contain autotrophs (e.g., phytoplankton) and heterotrophs (e.g., bacteria; Crane and Grover 2010, Cropp and Norbury 2015, Thingstad et al. 1996), leading to the prediction that mixotrophs should become dominant in ecosystems in which nutrients are limiting (Mitra et al. 2016). This prediction is consistent with the observation that mixotrophs are particularly abundant in open ocean oligotrophic gyres (Hartmann et al. 2012) and in coastal ecosystems where a single nutrient, such as phosphorus, is scarce (Burkholder et al. 2008). However, Rothhaupt (1996a) showed that the persistence of mixotrophs alongside strictly heterotrophic competitors depended upon the availability of light and food as joint-limiting resources.

Here, we instead focus on competition between mixotrophs and their intraguild prey for sunlight. In keeping with intraguild predation theory, mixotrophs should gain a competitive advantage when light is the sole limiting resource because, by consuming their phytoplankton competitors, they reduce competition for light. In this paper, we report on our test of this prediction using a combination of mathematical and experimental approaches. First, we constructed a mathematical model for the interaction of a phytoplankter (the intraguild prey) and a mixotroph (the intraguild predator) in a well-mixed water column with a single limiting resource (light). We evaluated how coexistence and competitive exclusion depend upon the strength of species interactions (i.e., intraguild predation) and upon ecosystem

productivity (i.e., the availability of sunlight). We then compared our theoretical results with experiments using two widely distributed marine planktonic taxa. Our analysis highlights the generality of intraguild predation as a mechanism for coexistence and enhanced diversity among organisms that share a resource niche.

The model

To study the effects of intraguild predation on the coexistence dynamics of two competing phytoplankton species, we modified the classic model of Huisman and Weissing (1994) for phytoplankton living in a well-mixed water column (i.e., each cell experiences, on average, the same amount of light). At a given depth z , the biomass-specific growth rate g_i of a phytoplankter of species i is determined by the difference between its photosynthetic rate, which is a function of its inherent maximum rate of carbon uptake via photosynthesis p_i and local light availability $I(z)$, and its respiration rate ℓ_i . Thus

$$g_i(z) = p_i \frac{I(z)}{h_i + I(z)} - \ell_i \quad (1)$$

where h_i is the light level at which half the maximum photosynthetic rate is achieved. (All variables and parameters are listed in Table 1).

Following Huisman and Weissing (1994), we assumed that available light declines with depth following the Lambert-Beer law and that each species has a per-cell light absorptivity k_i . Because the water column is well-mixed, the cell density w_i for each species does not depend on depth. As a result of absorption, the light intensity $I(z)$ decreases with depth from the incident level I_{in} at the surface according to

$$I(z) = I_{in} \exp[-(k_1 w_1 + k_2 w_2)z]. \quad (2)$$

Integrating over the total depth of the water column, the rate of change in each of the two species' total biomass W_1 and W_2 is given by

$$\frac{dW_1}{dt} = \frac{p_1 W_1}{k_1 W_1 + k_2 W_2} \ln \left[\frac{h_1 + I_{in}}{h_1 + I_{in} \exp[-(k_1 W_1 + k_2 W_2)]} \right] - \ell_1 W_1 \quad (3)$$

$$\frac{dW_2}{dt} = \frac{p_2 W_2}{k_1 W_1 + k_2 W_2} \ln \left[\frac{h_2 + I_{in}}{h_2 + I_{in} \exp[-(k_1 W_1 + k_2 W_2)]} \right] - \ell_2 W_2. \quad (4)$$

(See Huisman and Weissing 1994 for the complete derivation.) Thus, competition between the two phytoplankton species is mediated by competition for light.

We modified these equations to account for intraguild predation by allowing species 2 (now denoted M for “mixotroph”) to predate species 1 (denoted W , in

TABLE 1. Model symbols and their meanings.

Symbol	Description	Typical units	Simulation values
Variable			
W	Phytoplankton (intraguild prey)	cells/cm ²	
M	Mixotroph (intraguild predator)	cells/cm ²	
t	Time	d	
Parameter			
I_{in}	Surface (incoming) light intensity	μmol quanta · m ⁻² · s ⁻¹	Varied
p_w	Maximum carbon uptake rate, phytoplankter	d ⁻¹	1
p_m	Maximum carbon uptake rate, mixotroph	d ⁻¹	1, 0.3
k_w	Light absorbance of phytoplankter	cm ² cell _w ⁻¹	1 × 10 ⁻⁷
k_m	Light absorbance of mixotroph	cm ² cell _w ⁻¹	1 × 10 ⁻⁷ , 5 × 10 ⁻⁷
h_w	Half-saturation light intensity for phytoplankter	μmol quanta · m ⁻² · s ⁻¹	200
h_m	Half-saturation light intensity for mixotroph	μmol quanta · m ⁻² · s ⁻¹	200, 250
ℓ_w	Mortality rate of phytoplankter	d ⁻¹	0.05
ℓ_m	Mortality rate of mixotroph	d ⁻¹	0.05, 0.1
a	Attack rate of mixotroph on phytoplankter	μmol quanta · m ⁻² · s ⁻¹	Varied
b	Conversion rate of phytoplankter to mixotroph	cell _M cell _w ⁻¹	Varied

keeping with the Huisman and Weissing (1994) original notation for phytoplankton) with an attack rate a and biomass conversion efficiency b :

$$\frac{dW}{dt} = \frac{p_w W}{k_w W + k_m M} \ln \left[\frac{h_w + I_{in}}{h_w + I_{in} \exp[-(k_w W + k_m M)]} \right] - \ell_w W - aWM \quad (5)$$

$$\frac{dM}{dt} = \frac{p_m M}{k_w W + k_m M} \ln \left[\frac{h_m + I_{in}}{h_m + I_{in} \exp[-(k_w W + k_m M)]} \right] - \ell_m M + baWM. \quad (6)$$

Note that, for consistency with the Huisman & Weissing original formulation, the units of the attack rate a are in area per time per mixotroph (cm² · d⁻¹ · cell_M⁻¹; Table 1). Thus our model assumes that grazing is proportional to the integrated population sizes of the phytoplankter and the mixotroph, rather than to their population densities (i.e., that grazing is independent of mixed layer depth). However, in planktonic communities, grazing is likely to depend upon absolute concentration (i.e., in cells/mL). Thus, our model strictly applies only when the mixed layer depth does not change with time, as is the case in our subsequent analyses.

Analysis

Relative competition for light.—In Eqs. 5 and 6, the minimum surface light levels I_w and I_m required for the persistence of the phytoplankter and the mixotroph in monoculture are

$$I_w = \frac{\ell_w h_w}{p_w - \ell_w} \quad \text{and} \quad I_m = \frac{\ell_m h_m}{p_m - \ell_m}. \quad (7)$$

These light levels are called the “compensation irradiances” (sensu Huisman and Weissing 1994). As long as I_{in} exceeds either I_w or I_m , an isolated phytoplankton or mixotroph population, respectively, will grow when small.

Huisman and Weissing (1994) previous analysis of the pure competition model (Eqs. 3 and 4) showed that, except for special parameter combinations that produce functionally identical phytoplankton species, competition for light results in competitive exclusion at equilibrium. Specifically, each species when grown in monoculture reduces light at the bottom of the water column to a fixed, species-specific, value I_{out}^* . In two-species cases, the species with the lowest I_{out}^* outcompetes the other. There is no closed-form expression for I_{out}^* —it must be calculated numerically—but it depends upon all the model parameters except for light absorptivity. When phytoplankton differ in only one trait, the outcome is straightforward: the species with the highest photosynthetic rate, lowest half-saturation intensity, or lowest mortality rate is competitively dominant.

In our model (Eqs. 5 and 6), whenever the mixotroph M is the superior competitor, it competitively excludes the phytoplankter W as long as surface light I_{in} is sufficient for the mixotroph’s persistence. Therefore, we confined our analyses to the more dynamically interesting situation in which the phytoplankter W is the superior competitor (i.e., where $I_w < I_m$, or, equivalently, where all other parameters are equal and $p_w > p_m$ or $h_w < h_m$ or $\ell_w < \ell_m$). In this case, the persistence of the mixotroph M is promoted by its intraguild predation. This scenario is also likely to be the most biologically relevant because mixotrophs, which incur the increased metabolic costs of maintaining two forms of metabolic machinery (Raven 1997), are typically thought to be weaker competitors for light than phytoplankton (Skovgaard et al. 2000, Adolf et al. 2006, Crane and Grover 2010).

Model equilibria and their stability.—Our model (Eqs. 5 and 6) has four possible non-negative equilibria: $(0,0)$, at which no species are present; $(W^*, 0)$, at which only the phytoplankter persists; $(0, M^*)$, at which only the mixotroph persists; and (W^c, M^c) , at which the two species coexist.

The population dynamics of both species fundamentally depend upon the availability of light. When surface light I_{in} is lower than I_w , the no-species $(0,0)$ equilibrium is stable (because there is insufficient light for phytoplankton growth). With more light, the phytoplankter persists. Further increases in light produce coexistence of the phytoplankter and the mixotroph, and, ultimately, result in competitive exclusion of the phytoplankter by the mixotroph (Appendix S1; Fig. S1).

Transitions between the three positive equilibria also depend upon the species interaction parameters a and b , which determine the attack rate of the mixotroph, and the conversion efficiency from phytoplankton to mixotroph biomass, respectively (Fig. 1). For $I_{in} > I_m$ (i.e., surface light is sufficiently high that the mixotroph could persist in monoculture), the effects of a and b on the stability of equilibria can be understood by examining the relationship between the zero net growth isoclines (“nullclines”) for each species. These nullclines are determined by setting dW/dt and dM/dt equal to zero. There are two nullclines for the phytoplankter, defined by the equations $W = 0$ and

$$0 = \frac{P_w}{k_w W + k_m M} \ln \left[\frac{h_w + I_{in}}{h_w + I_{in} \exp[-(k_w W + k_m M)]} \right] - \ell_w - aM, \quad (8)$$

and two nullclines for the mixotroph, given by $M = 0$ and

$$0 = \frac{P_m}{k_w W + k_m M} \ln \left[\frac{h_m + I_{in}}{h_m + I_{in} \exp[-(k_w W + k_m M)]} \right] - \ell_m + baW. \quad (9)$$

These nullclines determine the regions in the phase plane for which each species experiences either positive or negative population growth. On the nullclines themselves, the species from whose equation the nullcline is derived does not grow, and thus the nullclines’ intersections represent the system’s equilibria. When $a = b = 0$, the interior (i.e., non-axis) nullclines are parallel (Huisman and Weissing 1994, fig. 4), leading to competitive exclusion by the phytoplankter because it has the greatest competitive ability for light. However, changing values of a and b can cause the interior nullclines to intersect up to two times, allowing for multiple stable states (Fig. 1, middle column).

The parameters a and b determine equilibrium stability through their effects on the shape of the nullclines. First, note that M^* , the monoculture abundance of the

mixotroph, is defined mathematically as the M -axis intercept of the M interior nullcline, found by setting $W = 0$ in Eq. 9. M^* is determined only by surface light I_{in} and the traits that govern the mixotroph’s photosynthetic growth, p_m , k_m , h_m , and ℓ_m ; it is independent of a and b because it is the abundance of the mixotroph in the absence of prey. The equilibrium point $(0, M^*)$ is stable when the M -intercept of the W interior nullcline is less than M^* . Because the latter intercept is controlled by a , we can define a^* mathematically by evaluating the W nullcline at $(0, M^*)$:

$$a^* = \frac{P_w}{k_m (M^*)^2} \ln \left[\frac{h_w + I_{in}}{h_w + I_{in} \exp(-k_m M^*)} \right] - \frac{\ell_w}{M^*}. \quad (10)$$

when $a > a^*$ (solid vertical line, left panel of Fig. 1), the equilibrium point $(0, M^*)$ is asymptotically stable. Thus a^* is the minimum attack rate above which the mixotroph M can, depending upon initial conditions, exclude the phytoplankter W (regions III–V, Fig. 1).

Second, the monoculture abundance of the phytoplankter, W^* , is defined as the W -axis intercept of the W interior nullcline, found by setting $M = 0$ in Eq. 8. As with M^* , W^* depends only on phytoplankter photosynthetic traits and surface light. The prey-only equilibrium point $(W^*, 0)$ is stable if the W -intercept of the M interior nullcline (which is also determined by a and b ; Fig. 1, middle column) is less than W^* . Therefore, for any given attack rate a , we can compute a conversion efficiency $b^*(a)$ at which the nullclines share a W -axis intercept. For the M nullcline, this intercept occurs at $(W^*, 0)$; thus, b^* must satisfy

$$0 = \frac{P_m}{k_w W^*} \ln \left[\frac{h_m + I_{in}}{h_m + I_{in} \exp(-k_w W^*)} \right] - \ell_m + b^* a W^*. \quad (11)$$

when $b > b^*(a)$ (dashed line, left panel of Fig. 1), the $(W^*, 0)$ equilibrium is unstable. In other words, $b^*(a)$ is the minimum conversion efficiency above which M invades and persists regardless of initial conditions (regions II, IV, and V, Fig. 1).

Finally, because b controls the curvature of the M interior nullcline, we define \hat{b} as the value of b at which the nullclines are just tangent to each other: that is, they transition from having two positive intersections to having none. Because the nullclines can only have two positive intersections (region IV, middle column of Fig. 1) when $a > a^*$, \hat{b} exists, and is a function of a , only when $a > a^*$. Biologically, $\hat{b}(a)$ (dotted line, left panel of Fig. 1) is the conversion efficiency above which M excludes W regardless of initial conditions (i.e., only the $(0, M^*)$ equilibrium is stable; region V, Fig. 1).

Because the model involves mixed exponentials, we solved for a^* , $b^*(a)$, and $\hat{b}(a)$ numerically for each set of parameters and used numerical simulations to check the asymptotic stability of predicted equilibria. We found that there are five distinct regions in the a - b plane

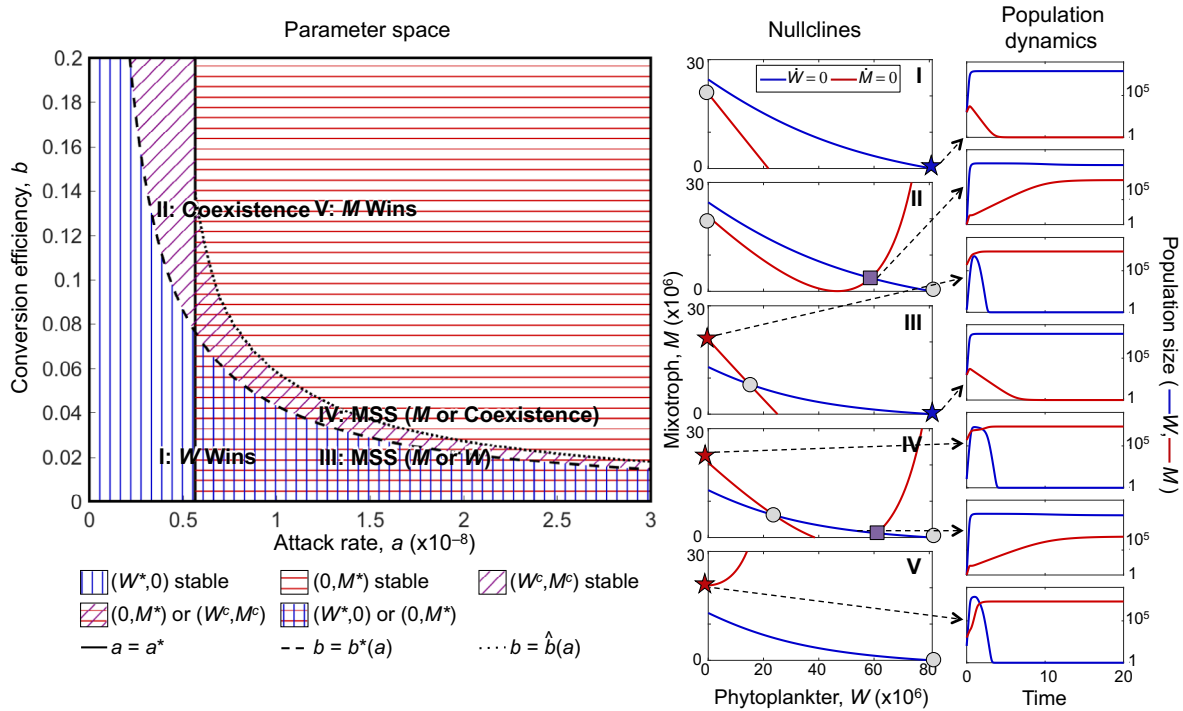


FIG. 1. The effect of species interaction parameters (attack rate a and conversion efficiency b) on equilibrium population outcomes. When attack rates are low ($a < a^*$), the phytoplankter always persists; for sufficiently high conversion efficiencies ($b > b^*(a)$), the phytoplankter and mixotroph coexist. When $a > a^*$, the asymptotic population dynamics depend upon b . As b increases, model stability transitions from bistability (either the phytoplankter or the mixotroph outcompetes the other, depending upon initial conditions) to a different type of bistability (either the mixotroph outcompetes the phytoplankter, or the two species coexist) to a single equilibrium point (the mixotroph outcompetes the phytoplankter). Roman numerals on the leftmost panel correspond to a and b parameter choices whose nullclines are displayed in the middle column. Stable equilibria are marked by colored symbols (blue stars = phytoplankter-only stable, red stars = mixotroph-only stable, purple squares = coexistence stable), with corresponding example population trajectories shown in the rightmost column. Positive, unstable equilibria are indicated by gray circles. Two nullclines ($W = 0$ and $M = 0$) and the unstable equilibrium at $(0, 0)$ are unmarked in each nullcline plot. Parameters are listed in Table 1, with $I_{in} = 100$, $p_m = 0.3$, $h_m = 200$, $k_m = 1 \times 10^{-7}$, and $\ell_m = 0.05$.

delimited by the curves $a = a^*$, $b = b^*(a)$, and $b = \hat{b}(a)$ (Fig. 1). Two of these regions exhibit bistability. That is, there are two asymptotically stable positive equilibrium points, and the dynamics of the system are therefore dependent upon initial conditions (Fig. 1, regions III and IV; see alternative population dynamics in the rightmost column and velocity diagrams and population trajectories in Appendix S1: Fig. S2).

The location and extent of these stability regions depends upon model parameters. For example, more surface light (larger I_{in}) increases the portion of a - b parameter space over which the mixotroph can persist and competitively exclude the phytoplankter (Fig. 2). Species traits, including half-saturation constants and mortality rates, affect the model’s sensitivity to a and b , but do not qualitatively change the trajectory of the system’s response to resource enrichment (Appendix S1: Fig. S3).

Empirical comparison

Collectively, our analysis of Eqs. 5 and 6, leads to two main predictions: (1) With increasing surface light levels,

mixotroph persistence should increase; and (2) with increasing attack rates, mixotroph persistence should also increase. Further, our model makes specific predictions about the number and stability of equilibria in the system for given sets of parameters. To test our model’s predictions, we developed a laboratory experimental system using mixotrophic and photosynthetic plankton, and manipulated light, attack rates, and initial conditions.

Study organisms and culture conditions.—Our laboratory experimental system used two taxa: *Micromonas comoda* (strain CCMP 2709; Van Baren et al. 2016, Worden et al. 2009), a cosmopolitan eukaryotic phytoplankter that is dominant in both coastal and oligotrophic ocean regions (Cottrell and Suttle 1991, Not et al. 2004), and *Ochromonas* sp. (strains CCMP 1391, 1393, and 2951), a mixotrophic chrysophyte (Rothhaupt 1996a). *Ochromonas*-like flagellates are important grazers in a variety of marine and freshwater environments. Because both *Ochromonas* and *Micromonas* are known to be bacterivorous (Sanders and Gast 2011, Wilken et al. 2013, McKie-Krisberg and Sanders 2014), we worked with axenic

cultures to ensure that growth was limited to phototrophy (both species) and intraguild predation (grazing of *Micromonas* by *Ochromonas*). Cultures CCMP 2709 and 1391 were ordered from the National Center for Marine Algae and Microbiota (NCMA, Bigelow Laboratory, East Boothbay, ME, USA), and CCMP 1393 and 2951 were provided by S. Wilken.

All stock cultures were maintained in K medium (Keller et al. 1987; see Table S1 for list of nutrient contents) made by adding pre-mixed nutrients (ordered from the NCMA) to 0.2 μm filtered Santa Barbara coastal seawater. Stock cultures were maintained in 40-mL tissue culture flask batch cultures at 24°C under a 12 h:12 h light:dark cycle with light illumination from above. We used mesh screening, in combination with varied shelf proximity to overhead light sources, to create three light environments (100, 50, and 20 $\mu\text{mol quanta} \cdot \text{m}^{-2} \cdot \text{s}^{-1}$) and acclimated cultures to their experimental light levels

for a period of at least 4 weeks prior to beginning any data collection. All cell enumeration was done by subsampling each culture for analysis by size and fluorescence on a Guava easyCyte flow cytometer (EMD Millipore, Darmstadt, Germany).

Quantifying relative photosynthetic growth rates.—To verify that our experimental system was appropriate to our mathematical model, we conducted a series of preliminary experiments. First, we grew both *Micromonas* and *Ochromonas* in isolation and compared their maximum photosynthetic growth rates. Growth rates were measured by inoculating cells at 2,000 cells/mL (*Ochromonas*) or 50,000 cells/mL (*Micromonas*) in triplicate, and quantifying population sizes for a period of up to 8 d. For each replicate, we calculated growth rate as the maximum slope of a semilog plot of population size vs. time. In some cases, this calculation required eliminating later (i.e., after

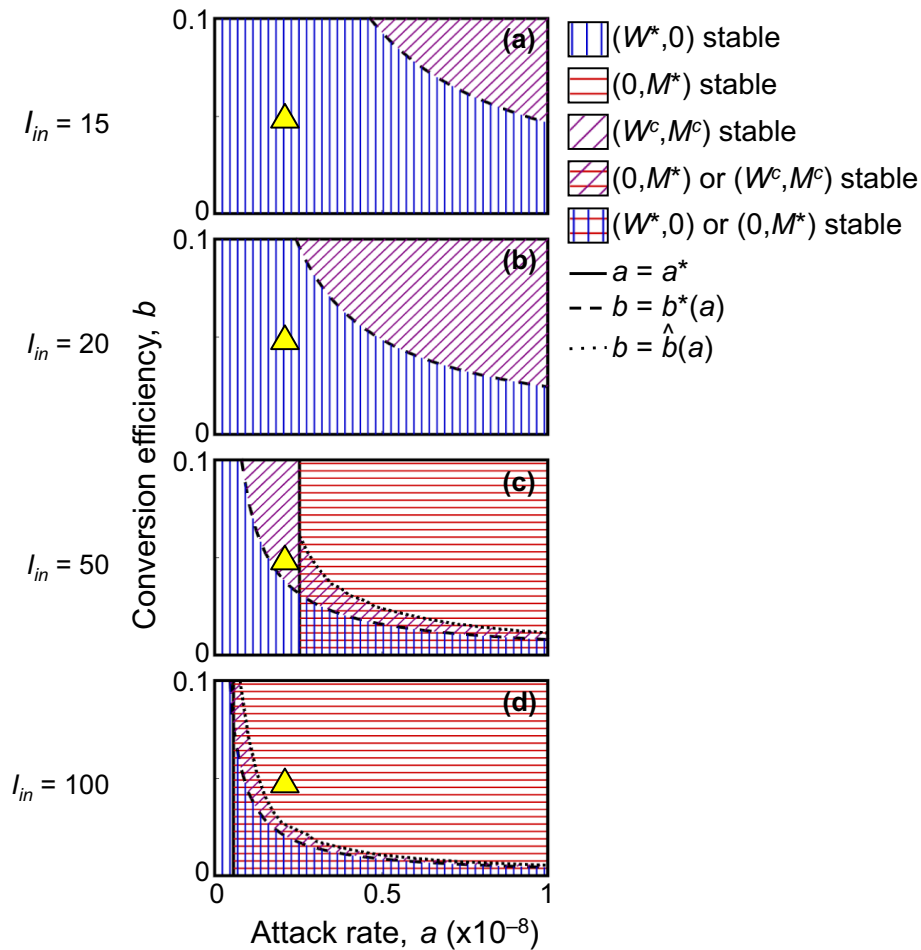


FIG. 2. Effect of changing light levels on equilibrium population outcomes. Each panel shows the stability of equilibria for a range of attack rates a and conversion coefficients b . Surface light increases from top to bottom. As the resource becomes more enriched (increasing light), the range of parameter space over which the mixotroph may persist increases. For example, the yellow triangles, which represent a system with $a = 2 \times 10^{-9}$ and $b = 0.05$, indicate that, as surface light increases, the system would transition from a phytoplankton-only equilibrium ($I_{in} = 15, 20$) to coexistence ($I_{in} = 50$) to mixotroph-only ($I_{in} = 100$). Equilibrium stability is indicated as in Fig. 1.

Day 6) time points because population growth slowed as populations approached carrying capacity. We defined maximum photosynthetic growth rate as the growth rate achieved at $100 \mu\text{mol quanta} \cdot \text{m}^{-2} \cdot \text{s}^{-1}$ (the highest light level). We found that the phytoplankter *Micromonas* had a growth rate approximately three times as high as the three mixotrophic *Ochromonas* strains (Fig. 3a; Appendix S1: Fig. S4). In this two-species system, as in our model analysis, the mixotroph is the weaker competitor for light.

Measuring a gradient of attack rates.—We used different strains of *Ochromonas* to manipulate the variable of attack rate. Because, to our knowledge, grazing of *Micromonas* by *Ochromonas* has not been previously reported, we first measured attack rates (i.e., grazing rates) in a separate experiment. To do this, we incubated *Micromonas* with and without *Ochromonas* at all three light levels and at three predator:prey ratios (1:10, 1:20, and 1:100, with a starting *Ochromonas* concentration of 2,000 cells/mL and a starting volume of 2 mL), and measured changes in population size over 24 h. Over this time period, prey were never completely extirpated, and the maximum decrease in prey abundance was by 50% from starting densities. Thus, it is unlikely that prey depletion caused an underestimation of *Ochromonas* attack rates. We used the equations of Frost (1972) and Heinbokel (1978) (developed in Jeong and Latz 1994) to calculate grazing rates for each of the three strains of *Ochromonas*. We found that *Ochromonas* did graze on *Micromonas*, with rates that differed consistently across strains and increased with increasing prey:predator ratios (Fig. 3b). We confirmed that grazing rates increased linearly with prey:predator ratio by fitting both linear (Holling Type I) and saturating (Holling Type II) models to the data, and comparing the associated values. AIC values were the same (CCMP 1391 and 1393) or lower (CCMP 2951) for the linear models, indicating that a linear (Type I) approximation was a good fit for our empirical system. Grazing was confirmed by using fluorescence microscopy to visualize *Micromonas* prey cells inside of *Ochromonas* digestive vacuoles, and by verifying that *Ochromonas* growth rates increased with increasing prey availability in later experiments (Appendix S1: Fig. S5). These data allowed us to manipulate the attack rate (i.e., a) by using three strains of *Ochromonas* with different grazing rates.

Testing for light limitation.—We verified that our system was light-limited by demonstrating that each organism's carrying capacity increased with increasing light availability. As part of our main experiment (details below) we measured carrying capacity as the maximum population size achieved by each taxon at each light level over a period of 20 ($100 \mu\text{mol quanta} \cdot \text{m}^{-2} \cdot \text{s}^{-1}$), or 40 d ($20 \mu\text{mol quanta} \cdot \text{m}^{-2} \cdot \text{s}^{-1}$). For *Ochromonas*, we included data in which *Micromonas* prey were initially available but were ultimately eliminated by grazing, because some *Ochromonas* strains have been shown to

have grazing-enhanced phototrophy (Lie et al. 2018). Indeed, we observed that two of our *Ochromonas* strains (CCMP 1393 and CCMP 2951) achieved higher population sizes when prey were available (Appendix S1: Fig. S7). Because carrying capacity increased with increasing light levels for all four taxa used in the study, we inferred that light was a limiting resource in our experimental system (Fig. 3c). However, we were surprised to note that, although increases in *Micromonas* populations with light were statistically significant, the magnitude of these changes was smaller than expected (approximately 5%). We also estimated absorption coefficients for each taxon by measuring light transmission through 1-cm of cultures of known concentration, and found that $k_w = 1 \times 10^{-7} \text{ cm}^2/\text{cell}$ and $k_m = 5 \times 10^{-7} \text{ cm}^2/\text{cell}$. We did not observe significant differences in absorption coefficients for cells acclimated to different light levels, or for fed vs. unfed mixotroph cells, so we pooled data across light levels. We used this information to select an experimental water column depth of 8 cm for our experimental test of model predictions.

We also tested for the role of other, potentially co-limiting resources in our experimental system. We verified that inorganic carbon was unlikely to be limiting by measuring pH of fresh media and of 30-d-old stock (non-experimental) cultures, and finding no significant difference (pH fresh: 8.41; pH old: 8.51 ± 0.05 ; $P = 0.129$, t -statistic = 1.811, $df = 5$). To prevent nutrients from becoming co-limiting during experiments, we ran our experimental test of model predictions in nutrient-rich 2K media (i.e., media with twice the nutrient content of K media; Keller et al. 1987). We used published estimates of cellular nitrogen content to estimate the N budget in our cultures (Appendix S1: Table S2) and found that at maximum population densities, *Micromonas* and *Ochromonas* would use approximately 4–20% of the available N in the 2K culture medium respectively (Appendix S1: Table S3). We also performed a separate experiment in which we tested for the effects of nutrients on carrying capacity by growing *Micromonas* at $50 \mu\text{mol quanta} \cdot \text{m}^{-2} \cdot \text{s}^{-1}$ in media with half (K/2), full (K), double (2K), or quadruple (4K) the nutrient content of K media, and found that carrying capacity was not significantly affected by nutrient content (Appendix S1: Fig. S6).

Generation of comparable model and experimental data.—We used data on species traits to determine the appropriate qualitative comparisons between our mathematical and empirical systems. Specifically, we modeled the expected dynamics for varied surface light I_{in} and attack rates a given other parameters chosen based on empirical data: $p_m = 0.3$ (i.e., the photosynthetic growth rate of the mixotroph was 30% that of the phytoplankter), $h_m = 250$ (i.e., the half-saturation irradiance of the mixotroph was larger than that of the phytoplankter), $k_m = 5 \times 10^{-7}$ (i.e., the absorptivity of the mixotroph was five times that of the phytoplankter), and $\ell_m = 0.1$

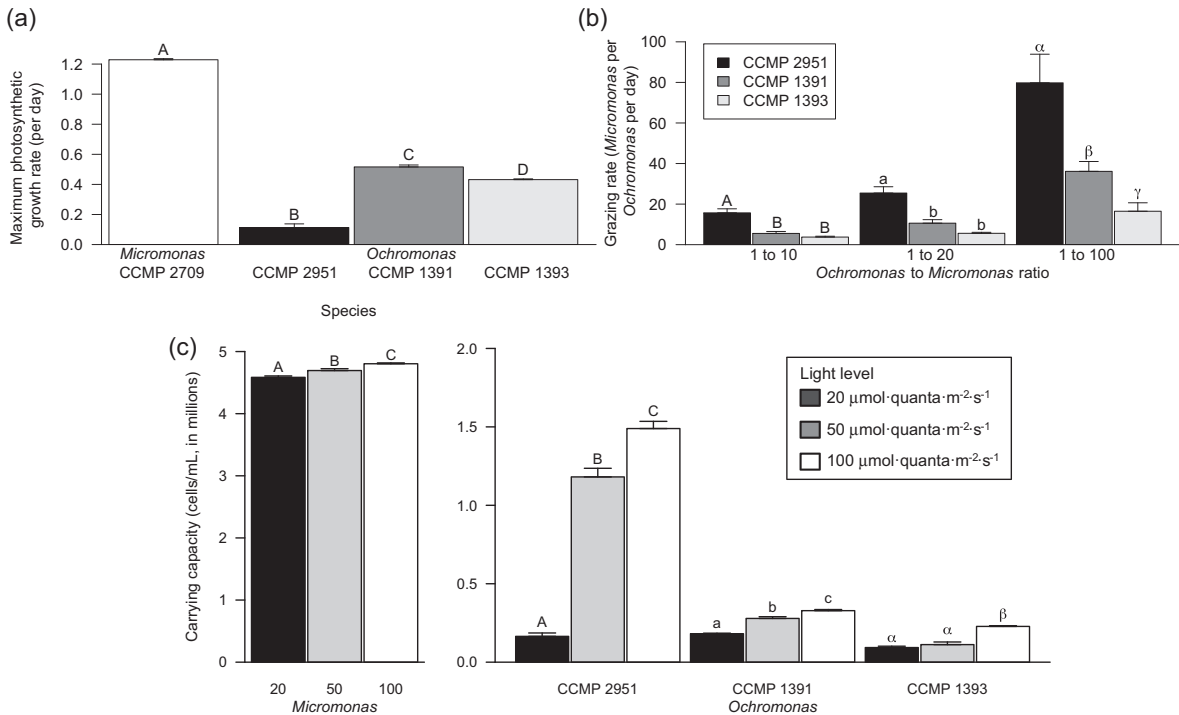


FIG. 3. Traits of the four experimental organisms. Panel A: The phytoplankter *Micromonas* CCMP 2709 exhibited a significantly greater maximum photosynthetic growth rate than the three mixotrophic *Ochromonas* strains CCMP 1391, 2951, and 1393 ($P < 0.01$, Tukey’s [honestly significant difference]); the three *Ochromonas* strains also differed, though not as substantially, from one another ($P < 0.05$, Tukey’s HSD). Data are from pilot experiments. Panel B: The three *Ochromonas* strains differed in their grazing rates, with strain 2951 exhibiting the highest grazing rates, and strain 1393 the lowest. Note that empirically measured grazing rates are equivalent to aM (the product of the mathematical model’s attack rate and the population of *Micromonas*). To convert between grazing rates and attack rates used in the mathematical model, one must divide by the population size of *Micromonas*. Grazing rates increased with increasing initial prey concentrations. Letters indicate significant differences at the $P < 0.05$ level (Tukey’s HSD comparing grazing rates grouped by prey concentration). Data are from pilot experiments. Panel C: Carrying capacities of the four experimental organisms as a function of light level. Both *Micromonas* (left) and the three *Ochromonas* strains (right) exhibited increasing maximum population sizes with increasing input light (Tukey’s HSD comparing population size grouped by species; letters indicate significant differences at the $P < 0.05$ level). Data are from the main experiment.

(i.e., the intrinsic mortality rate of the mixotroph was twice that of the phytoplankter). Thus, unlike in our strictly theoretical exploration (Figs. 1, 2, Appendix S1: Fig. S3) in which we varied traits independently, our empirical data suggested that *Ochromonas* strains were competitively inferior to *Micromonas* because of simultaneous differences in multiple traits. We varied light intensity and attack rate over parameter ranges that captured the most dynamically interesting regions of parameter space; in both cases, this meant varying these parameters over ranges that were greater than in our empirical system.

For a given attack rate, our model predicted transitions from phytoplankton-dominated to mixotroph-dominated equilibria with increasing surface light (Fig. 4). The sequence of transitions depends upon attack rate: For relatively low values of a , increasing light should cause systems to transition from phytoplankter-only, to bistability of single-species equilibria, to bistability of coexistence and mixotroph-only, to mixotroph-only states. For higher values of a , there is no

bistability of single-species equilibria (Fig. 4). Furthermore, in regions of bistability, increasing surface light reduces the basin of attraction for the coexistence equilibrium (Fig. 4, compare panels II and III), meaning that a wider range of initial conditions should lead to exclusion of the phytoplankter by the mixotroph.

We tested this prediction by generating time series population data on *Ochromonas* and *Micromonas* in co-culture. We manipulated the availability of light, the limiting resource, using mesh screens as described above, and manipulated attack rate by using three strains of *Ochromonas*. Because our mathematical model predicted bistability for some parameter combinations, we also varied experimental initial conditions by initiating experiments with 1:10, 1:20, or 1:100 ratios of *Ochromonas* to *Micromonas*. For example, when the initial density of *Ochromonas* was 2,000 cells/mL, we initialized *Micromonas* at 20,000, 40,000, or 200,000 cells/mL. To verify that experimental conditions were viable for population growth of *Micromonas* in the absence of competition, we also set up three *Ochromonas*-free controls with initial

abundances of 20,000, 40,000, or 200,000 *Micromonas* cells/mL. Note that some variation in initial abundances did occur, but ratios were held constant.

For each parameter and initial condition combination (3 light levels \times 3 attack rates \times 3 initial conditions = 27 treatments), we grew *Ochromonas* and *Micromonas* together in co-culture and collected population size data at intervals of one ($100 \mu\text{mol quanta} \cdot \text{m}^{-2} \cdot \text{s}^{-1}$), two ($50 \mu\text{mol quanta} \cdot \text{m}^{-2} \cdot \text{s}^{-1}$), or three ($20 \mu\text{mol quanta} \cdot \text{m}^{-2} \cdot \text{s}^{-1}$) days until the populations reached equilibrium sizes (20, 30, and 40 d, respectively). Each treatment and control was run in triplicate. Each experimental replicate contained a 10-mL semi-continuous batch culture in a 14-mL culture tube. Although the sides of the tubes were clear, cultures were illuminated from above to improve model-experiment agreement. Batch cultures were initialized by inoculating sterile media with a known concentration of *Micromonas* and/or *Ochromonas*. At each sampling point, cultures were mixed thoroughly by inversion, and a 250 μL sample was removed for flow cytometry enumeration. Culture volume was then replenished by adding 275 μL of fresh 2K media (the extra 25 μL compensated for low levels of evaporation); this corresponded to low dilution rates of 0.0275 (at high light) to 0.009 (at low light) per day.

Experimental data are consistent with model predictions.—Our population time series data qualitatively support model predictions. At the lowest attack rate (CCMP 1393, leftmost column of Fig. 5), as surface light increased, observed population dynamics transitioned from a *Micromonas*-only equilibrium to bistability between *Micromonas*-only and *Ochromonas*-only equilibria. At higher attack rates (CCMP 1391 and 2951, center and rightmost columns of Fig. 5, respectively), increasing light drove a transition from coexistence, to bistability between coexistence and an *Ochromonas*-only equilibrium (Fig. 5; see also Appendix S1: Figs. S7 and S8 for individual replicate time series data). Furthermore, comparisons of initial condition-dependence between intermediate and high light levels suggest that, consistent with model predictions, the basins of attraction for *Ochromonas*-only equilibria are growing with increasing light (Fig. 5, compare top and middle rows).

However, some interesting contrasts between our empirical and mathematical models emerged. First, our empirical results indicate that at low light levels and intermediate attack rates, the *Micromonas*-only and coexistence equilibria were simultaneously stable (Fig. 5, middle of bottom row). This contradicted our mathematical model, which did not predict the simultaneous stability of this pair of equilibria. Second, our empirically observed I_{out} light levels at the base of the experimental water columns were more variable than the model's predictions (Appendix S1: Fig. S9). Because our experimental water columns were not amenable to direct measurements using our light meter, we instead calculated I_{out} by multiplying taxon-specific absorptivities by

population densities at the final time point and the 8 cm water column depth. Although *Micromonas* control and *Micromonas*-only populations consistently drew I_{out} down to low levels, there were no significant differences among I_{out} levels (Appendix S1: Fig. S9), in contrast to a predicted decrease in I_{out} with increasing I_{in} (Huisman and Weissing 1994), empirically demonstrated by Huisman 1999). This was due to the relatively small population response of *Micromonas* to increasing light levels (Fig. 3c), which may indicate that, despite our other measurements, *Micromonas* experienced limitation by a non-light resource in some of the experiments. Overall, trends for *Ochromonas*-only and coexistence equilibria followed model predictions, with increasing I_{out} levels for coexistence equilibria as attack rates increased (Appendix S1: Fig. S9). However, *Ochromonas* population sizes were sometimes low (Appendix S1: Fig. S7), which contributed to divergence from model predictions (especially for prey-free treatments).

DISCUSSION

Using a mathematical model for mixotrophy grounded in resource competition theory, we demonstrated that two plankton species may coexist even when competing for a single limiting resource (light). Consistent with other forms of intraguild predation (Holt and Polis 1997, Mylius et al. 2001), mixotrophy permits the persistence of a weaker competitor for light that would otherwise be competitively excluded (Huisman and Weissing 1994). Our results complement the mathematical modeling work of Thingstad et al. (1996), who also showed that mixotrophs can coexist alongside their prey when competing for a limiting resource (in their case, nutrients). However, coexistence is not guaranteed: If the mixotroph has a high attack rate or conversion efficiency, or if surface light intensity is high, the mixotroph can exclude the phototroph. This is in keeping with other theoretical results that predict mixotroph dominance in high-resource environments (Wilken et al. 2014a, Ptacnik et al. 2016) such as eutrophic freshwater, estuarine, and coastal marine ecosystems.

Our experimental study qualitatively supported our mathematical model's predictions, with the mixotroph *Ochromonas* becoming more dominant (i.e., more likely to exclude the phytoplankter *Micromonas*) with increasing surface light intensity and increasing attack rates. The increasing dominance of the mixotroph as ecosystem productivity increased is consistent with a number of empirical studies of intraguild predator abundance in protistan (Morin 1999, Diehl and Feissel 2001, Price and Morin 2004) and insect (Borer et al. 2003) systems. We observed all three types of non-negative model equilibria (phytoplankter-only, mixotroph-only, and coexistence) and five types of model dynamics (monostability of each of the equilibria, simultaneous stability of the phytoplankter-only and mixotroph-only equilibria, and simultaneous stability of the coexistence and mixotroph-only

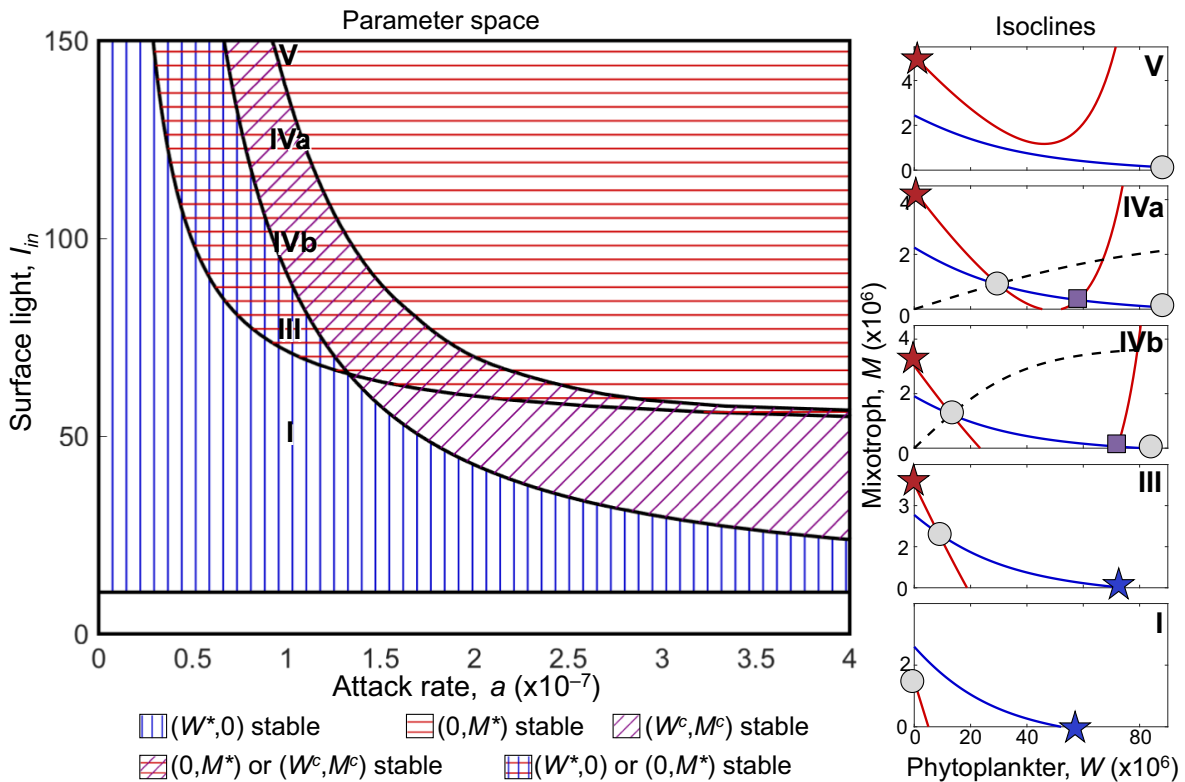


FIG. 4. Dependence of mathematical model predicted dynamics on surface light I_{in} and attack rate a . Legends and notation as in Fig. 1. As available light increases, the system transitions from competitive exclusion by prey, to alternate competitive exclusion states or coexistence, to bistability of coexistence and competitive exclusion by the mixotroph, and finally to competitive exclusion by the mixotroph. Nullclines are shown for increasing values of I_{in} at a fixed value of $a = 1 \times 10^{-7}$ (right column); Roman numerals are used to indicate specific parameter values and are chosen for consistency with Roman numerals in Fig. 1. Note that the basins of attraction for the bistable equilibria shift. For example, as I_{in} increases, the basin of attraction for the coexistence equilibrium (purple square) shrinks (nullclines corresponding to locations IVa and IVb). Parameters are as listed in Table 1, with $p_m = 0.3$, $h_m = 250$, $\ell_m = 0.1$, $k_m = 5 \times 10^{-7}$, and $b = 0.005$.

equilibria). Surprisingly, we also observed simultaneous stability of the phytoplankter-only and coexistence equilibria (Fig. 5, middle column of bottom row), which was not predicted by our mathematical model. We postulate that this outcome (in which *Micromonas* competitively excluded *Ochromonas* when it was inoculated at the highest population densities) may have resulted from stochastic extinction of a small population of *Ochromonas* as the populations dynamically approached equilibrium.

The Huisman and Weissing (1994) model for competing phytoplankton also allows for competitive outcomes to depend upon the productivity of an ecosystem. In their model, when phytoplankton differ in multiple traits (e.g., one species has a larger photosynthetic rate and a higher half-saturation light intensity than the other), the competitively dominant species may change as incoming light levels increase. In our analysis, we focused only on single-trait differences that result in productivity-independent competitive dominance for the phytoplankter. This allowed us to highlight the role that intraguild predation plays in permitting persistence in spite of

competitive inferiority. We expect that expanding our analysis to allow tradeoffs among species' traits would also reveal a complex dependence of competitive superiority on productivity, consistent with Huisman and Weissing (1994). For example, coexistence may also be mediated by divergent use of light [e.g., by maintaining photosynthetic pigments with absorption spectra that are maximized at different wavelengths; Stomp et al. 2004] and nutrient resources (e.g., by contrasting nutrient use efficiencies, but see Passarge et al. 2006). Furthermore, in the Huisman and Weissing (1994) analysis, outcomes could be predicted on the basis of I_{out}^* (which is inversely proportional to I_{in}) measured on each competitor in monoculture. In contrast, in our study, the mixotroph may competitively exclude the phytoplankter even when, in monoculture, its I_{out}^* is greater, because it is also able to feed on the phytoplankter (Appendix S1: Fig. S9). Because competition for light is mediated by standing stock biomass rather than production of new biomass, the competitive interactions between mixotrophs and phytoplankton mimic interference competi-

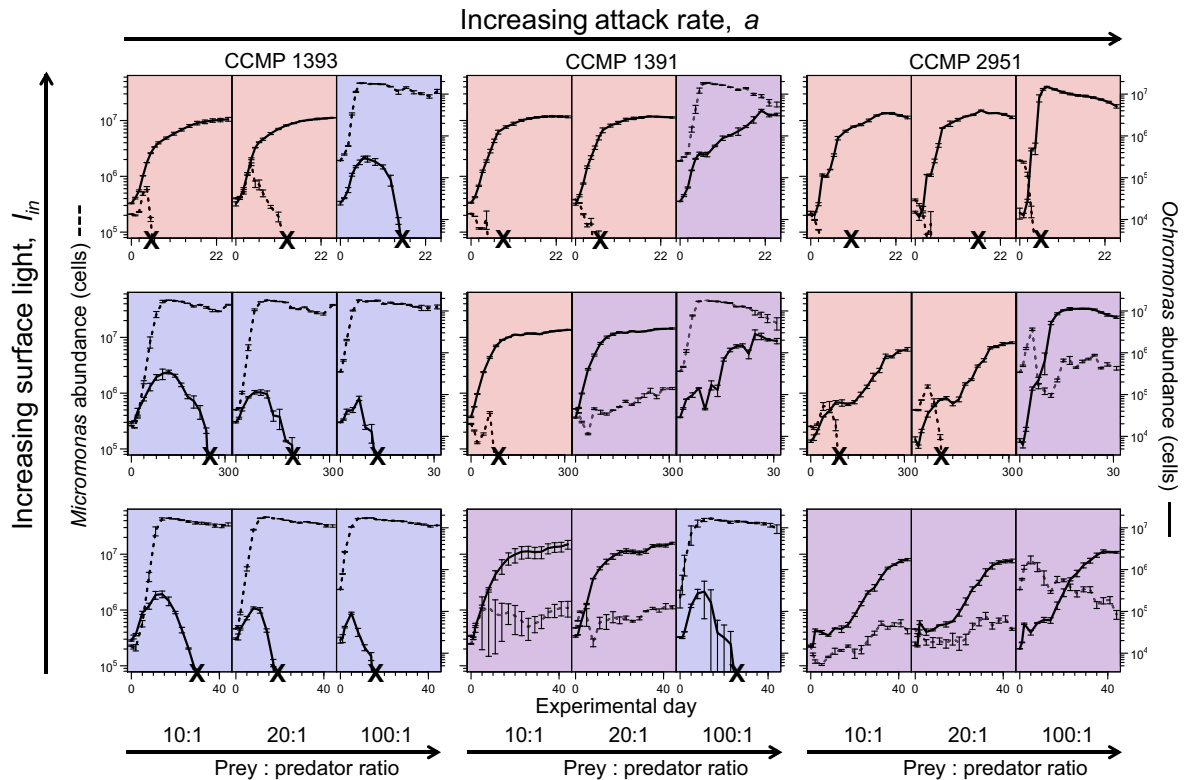


Fig. 5. Empirical test of model predictions. We experimentally manipulated light (by conducting experiments at three different light levels, top row = 100, middle row = 50, and bottom row = 20 $\mu\text{mol quanta} \cdot \text{m}^{-2} \cdot \text{s}^{-1}$), attack rate (by using three different *Ochromonas* strains, left column = CCMP 1393 with the lowest attack rate, right column = CCMP 2951 with the highest attack rate), and initial conditions (subplots grouped in threes, with initial conditions of 1:10, 1:20, and 1:100 *Ochromonas*:*Micromonas* from left to right). Time series of mean population sizes with standard errors are plotted for the mixotroph *Ochromonas* (solid lines) and the phytoplankter prey *Micromonas* (dashed lines). Y-axes (log scale) are the same for all plots. Extinctions are marked with an “X,” and subplot background color indicates the type of equilibrium observed (blue = phytoplankter only, red = mixotroph only, and purple = coexistence). Our data show a transition from *Micromonas*-dominated equilibria (phytoplankter-only and simultaneous stability of alternate competitive exclusion) to *Ochromonas*-dominated equilibria (mixotroph-only and simultaneous stability of mixotroph-only and coexistence) as grazing rates and light levels increase (from lower left to upper right). This is qualitatively consistent with the mathematical model predictions presented in Fig. 4.

Fig. 1) therefore allows for coexistence under specific ranges of parameter values.

The outcomes of our laboratory experiment also differed from model predictions in ways that illustrated the importance of grazing to mixotroph growth. For example, we found that *Ochromonas* strains CCMP 1393 and 2951 often attained higher population sizes when grown with *Micromonas* prey than when grown in isolation, even if they subsequently competitively excluded *Micromonas* (Fig. 5 and Appendix S1: Fig. S7). This had implications for light transmission (I_{out}), as light transmission for mixotroph-only equilibria tended to be higher than model predictions (Appendix S1: Fig. S9). Although all three strains used in this study were capable of transiently sustaining photosynthetic growth in the absence of prey (Fig. 3), other studies have shown that prey can enhance mixotroph photosynthetic capacity, perhaps by providing nutrients inaccessible in the culture media (Sanders et al. 2001, Lie et al. 2018).

Our goal in this study was to develop and test a model with a very general representation of intraguild predation among competitors competing for light as a single, shared limiting resource. Therefore, in our mathematical model, we disregarded the possibility of other limiting resources, such as nutrients, in our system. Although we did not measure nutrient levels over the course of our study, several lines of evidence indicate that light was the major limiting factor in our system. First, we initiated the experimental cultures with high concentrations of nutrients in the media (Appendix S1: Table S1; Keller et al. 1987) relative to estimated cellular quotas (Appendix S1: Table S3). Second, carrying capacity increased with increasing light availability (Fig. 3c) but was insensitive to media type (Appendix S1: Fig. S6). Finally, existing photophysiological studies of *M. commoda* (Thompson et al. 1991) and *Ochromonas* (Wilken et al. 2013) indicate that growth rates are light limited at irradiances below 100 $\mu\text{mol quanta} \cdot \text{m}^{-2} \cdot \text{s}^{-1}$ in both

taxa. The qualitative agreement between our mathematical and empirical systems suggests that, indeed, the single-resource model captured a core phenomenon about the experimental system. However, transcriptomic data suggest that *Ochromonas* strain CCMP 1393 may not be capable of using nitrate (Lie et al. 2018), which was the most abundant source of inorganic nitrogen in our culture medium (Appendix S1: Table S1). If strains preferentially utilized ammonium, this form of nitrogen could have been completely depleted (Appendix S1: Table S3), potentially causing the mixotrophs to function more like strict predators and promoting coexistence (Wilken et al. 2014b).

Incorporating co-limitation by nutrients (Stickney et al. 1999, Crane and Grover 2010), as well as other more complex mechanisms of species interactions such as alternate predation functional responses (Holling 1959), and light-dependence of photosynthetic (Flynn and Hansen 2013) and grazing rates (Skovgaard 1996, Holen 1999, Strom 2001), could improve the predictive abilities of a model for a specific system. For example, although in our study grazing rates did not systematically increase with increasing light (sensu Strom 2001; see Appendix S1: Fig. S10, especially higher prey ratios), correlations between attack rates and surface light would accelerate the transition to mixotroph-dominated equilibria. Our approach also does not account for changes in physiology under resource-limited conditions, such as photoacclimation (Herzig and Dubinsky 1992) or shifts in reliance on different forms of metabolism under different light regimes (Mitra et al. 2016).

Our *Ochromonas* strains did not exhibit a clear trade-off between investing in phototrophic vs. heterotrophic metabolisms that has been hypothesized to constrain mixotroph ecology: Although strain CCMP 2951 had the highest grazing rate and lowest photosynthetic rate, CCMP 1391 had the second highest grazing rate, yet highest photosynthetic rate (Fig. 3). Further, strain CCMP 2951 achieved the highest mixotrophic growth rates, but did so at intermediate light levels (Appendix S1: Fig. S5). These results highlight the complexities of real mixotroph physiology, wherein different taxa may derive different forms and degrees of benefit from ingesting prey (Mitra et al. 2016, Lie et al. 2018). Mixotrophs are also known to adjust their metabolic strategy as a function of environmental conditions: In addition to photoacclimation responses to different light levels, mixotrophs may downregulate photosynthetic machinery in the presence of high prey abundances (Sanders et al. 1990, Holen 1999, Wilken et al. 2013, 2014b). Such a response would cause *Ochromonas* to function more like a predator than a competitor, potentially altering dynamic outcomes, and/or accelerating extirpation of the prey. However, though we did not quantify cellular chlorophyll-*a* content or other photophysiological parameters, we observed no differences in either per-cell absorption coefficients or red fluorescence (a proxy for photosynthetic pigment content, measured by the flow

cytometer) for *Ochromonas* regardless of light and prey environment. One possible explanation is that undigested *Micromonas* chlorophyll inside of *Ochromonas* digestive vacuoles may have increased per-mixotroph pigment estimates, countering reductions in chlorophyll production by *Ochromonas*. Additional experiments would be needed to test this hypothesis.

In the course of our experiments, we obtained, to our knowledge, the first measurements of marine *Ochromonas* grazing on a eukaryotic phytoplankter, though such observations have been made on freshwater strains (Boraas et al. 1992). Both *Micromonas commoda* and *Ochromonas* are important in planktonic food webs. *Ochromonas* has long been recognized as a bacterivore that can exert top-down control on cyanobacteria (Wilken et al. 2014a) and heterotrophic bacteria (Katechakis and Stibor 2006), allowing it to outcompete strict heterotrophs (Rothhaupt 1996a, Katechakis and Stibor 2006). *Micromonas* is a cosmopolitan eukaryotic phytoplankter that may be dominant in both coastal and open-ocean settings (Cottrell and Suttle 1991, Not et al. 2004). The two species have been observed to co-occur at high abundances (Furuya and Marumo 1983), though no studies of potential grazing interactions have yet been conducted. Because the relative contribution of heterotrophy to *Ochromonas* metabolism is expected to increase with warming surface ocean temperatures (Wilken et al. 2013), understanding the breadth of this mixotroph's potential prey will be critical to predicting changes to planktonic production and nutrient cycling.

A number of theoretical studies have considered the role of constitutive mixotrophy, more generally, in constraining the dynamics and function of planktonic communities. By providing intermediate linkages within and between food chains, mixotrophs may serve as stabilizers of community dynamics (Jost et al. 2004, Hammer and Pitchford 2005) and as important mediators of the transfer of primary production to higher trophic levels (Ptacnik et al. 2004) and, potentially, carbon export (Ward and Follows 2016). Their generalist metabolic strategy also makes them more likely to dominate late-successional communities (i.e., late-season, stratified water columns) where nutrients have been depleted (Stickney et al. 1999, Mitra et al. 2014). Non-constitutive mixotrophs (which obtain their photosynthetic abilities from their prey) may also coexist with stronger competitors, sometimes creating cyclic, bloom dynamics with pulsed biogeochemical impacts (Moeller et al. 2016); in contrast to the constitutive mixotrophs in our *Ochromonas*–*Micromonas* system, however, these taxa cannot competitively exclude their prey because they rely on them as a source of photosynthetic machinery (Moeller et al. 2016).

In conclusion, by functioning as intraguild predators, mixotrophs that eat phytoplankton can coexist with these phytoplankton, even when the mixotrophs are the weaker competitor for the single limiting resource of light. Our results provide further evidence that, across

aquatic and terrestrial systems, from microscopic to macroscopic organisms, intraguild predator persistence is mediated by resource supply levels and the strength of species interactions. These observations are consistent with the omnipresence of mixotrophs in the world's marine and freshwater systems.

ACKNOWLEDGMENTS

HVM and MGN designed the model. HVM and MDJ designed the experimental test system. HVM performed the model analysis, conducted the experiments, and analyzed the data. All authors wrote the paper. We thank Susanne Wilken for generously providing axenic CCMP 2951 and 1393 cultures for our use. R. Germain, S. Louca, G. Owens, N. Sharp, P. Thompson, and J. Yoder provided valuable feedback on figure design. We also thank J. Bronstein, S. Diehl, J. Huisman, C. Klausmeier, and four anonymous reviewers for comments on earlier versions of this manuscript. HVM was supported by a United States National Science Foundation Postdoctoral Research Fellowship in Biology (Grant DBI-1401332) and a University of British Columbia Biodiversity Research Centre Postdoctoral Fellowship. This material is based upon work supported by the National Science Foundation under Grants OCE-1655686 and OCE-1436169, by a grant from the Simons Foundation/SFARI (561126, HMS), and by the Woods Hole Oceanographic Institution's Investment in Science Program. Research was also sponsored by the U.S. Army Research Office and was accomplished under Cooperative Agreement Number W911NF-19-2-0026 for the Institute for Collaborative Biotechnologies.

LITERATURE CITED

- Adolf, J. E., D. Stoecker, and L. W. Harding Jr. 2006. The balance of autotrophy and heterotrophy during mixotrophic growth of *Karlodinium micrum* (Dinophyceae). *Journal of Plankton Research* 28:737–751.
- Arim, M., and P. A. Marquet. 2004. Intraguild predation: a widespread interaction related to species biology. *Ecology Letters* 7:557–564.
- Boraas, M. E., D. B. Seale, and D. Holen. 1992. Predatory behavior of *Ochromonas* analyzed with video microscopy. *Archiv Hydrobiologie* 123:459–468.
- Borer, E. T., C. J. Briggs, W. W. Murdoch, and S. L. Swarbrick. 2003. Testing intraguild predation theory in a field system: Does numerical dominance shift along a gradient of productivity? *Ecology Letters* 6:929–935.
- Burkholder, J. M., P. M. Glibert, and H. M. Skelton. 2008. Mixotrophy, a major mode of nutrition for harmful algal species in eutrophic waters. *Harmful Algae* 8:77–93.
- Cottrell, M. T., and C. A. Suttle. 1991. Wide-spread occurrence and clonal variation in viruses which cause lysis of a cosmopolitan, eukaryotic marine phytoplankter *Micromonas pusilla*. *Marine Ecology Progress Series* 78:1–9.
- Crane, K. W., and J. P. Grover. 2010. Coexistence of mixotrophs, autotrophs, and heterotrophs in planktonic microbial communities. *Journal of Theoretical Biology* 262:517–527.
- Cropp, R., and J. Norbury. 2015. Mixotrophy: the missing link in consumer-resource-based ecologies. *Theoretical Ecology* 8:245–260.
- Diehl, S., and M. Feissel. 2001. Intraguild prey suffer from enrichment of their resources: a microcosm experiment with ciliates. *Ecology* 82:2977–2983.
- Fedriani, J. M., T. K. Fuller, R. M. Sauvajot, and E. C. York. 2000. Competition and intraguild predation among three sympatric carnivores. *Oecologia* 125:258–270.
- Flynn, K. J., and P. J. Hansen. 2013. Cutting the canopy to defeat the “Selfish Gene”: conflicting selection pressures for the integration of phototrophy in mixotrophic protists. *Protist* 164:811–823.
- Frost, B. W. 1972. Effects of size and concentration of food particles on the feeding behavior of the marine planktonic copepod *Calanus pacificus*. *Limnology and Oceanography* 17:805–815.
- Furuya, K., and R. Marumo. 1983. The structure of the phytoplankton community in the subsurface chlorophyll maxima in the western North Pacific Ocean. *Journal of Plankton Research* 5:393–406.
- Hammer, A. C., and J. W. Pitchford. 2005. The role of mixotrophy in plankton bloom dynamics, and the consequences for productivity. *ICES Journal of Marine Science* 62:833–840.
- Hartmann, M., C. Grob, G. A. Tarran, A. P. Martin, P. H. Burkhill, D. J. Scanlan, and M. V. Zubkov. 2012. Mixotrophic basis of Atlantic oligotrophic ecosystems. *Proceedings of the National Academy of Sciences of the United States of America* 109:5756–5760.
- Heinbokel, J. F. 1978. Studies on the functional role of tintinids in the Southern California Bight. I. Grazing and growth rates in laboratory cultures. *Marine Biology* 47:177–189.
- Herzig, R., and Z. Dubinsky. 1992. Photoacclimation, photosynthesis, and growth in phytoplankton. *Israel Journal of Botany* 41:199–212.
- Holen, D. A. 1999. Effects of prey abundance and light intensity on the mixotrophic chrysophyte *Poterioochromonas malhamensis* from a mesotrophic lake. *Freshwater Biology* 42:445–455.
- Holling, C. S. 1959. Some characteristics of simple types of predation and parasitism. *The Canadian Entomologist* 91:385–398.
- Holt, R. D., and G. A. Polis. 1997. A theoretical framework for intraguild predation. *American Naturalist* 149:745–764.
- Huisman, J. 1999. Population dynamics of light-limited phytoplankton: microcosm experiments. *Ecology* 80:202–210.
- Huisman, J., and F. J. Weissing. 1994. Light-limited growth and competition for light in well-mixed aquatic environments: an elementary model. *Ecology* 75:507–520.
- Hutchinson, G. E. 1941. Ecological aspects of succession in natural populations. *American Naturalist* 75:406–418.
- Hutchinson, G. E. 1961. The paradox of the plankton. *American Naturalist* 95:137–145.
- Jeong, H. J., and M. I. Latz. 1994. Growth and grazing rates of the heterotrophic dinoflagellates *Protoperidinium* spp. on red tide dinoflagellates. *Marine Ecology Progress Series* 106:173–185.
- Jost, C., C. A. Lawrence, F. Campolongo, W. van de Bund, S. Hill, and D. L. DeAngelis. 2004. The effects of mixotrophy on the stability and dynamics of a simple planktonic food web model. *Theoretical Population Biology* 66:37–51.
- Katechakis, A., and H. Stibor. 2006. The mixotroph *Ochromonas tuberculata* may invade and suppress specialist phago- and phototroph plankton communities depending on nutrient conditions. *Oecologia* 148:692–701.
- Keller, M. D., R. C. Selvin, W. Claus, and R. R. L. Guillard. 1987. Media for the culture of oceanic ultraphytoplankton. *Journal of Phycology* 23:633–638.
- Lie, A. A.-Y., Z. Liu, R. Terrado, A. O. Tatters, K. B. Heidelberg, and D. A. Caron. 2018. A tale of two mixotrophic chrysophytes: insights into the metabolisms of two *Ochromonas* species (Chrysophyceae) through a comparison of gene expression. *PLoS ONE* 13:e0192439-20.
- Maat, D. S., K. J. Crawford, K. R. Timmermans, and C. P. D. Brussaard. 2014. Elevated CO₂ and phosphate limitation favor *Micromonas pusilla* through stimulated growth and

- reduced viral impact. *Applied and Environmental Microbiology* 80:3119–3127.
- McKie-Krisberg, Z. M., and R. W. Sanders. 2014. Phagotrophy by the picoeukaryotic green alga *Micromonas*: implications for Arctic Oceans. *The ISME Journal* 8:1953–1961.
- Mitra, A., et al. 2014. The role of mixotrophic protists in the biological carbon pump. *Biogeosciences* 11:995–1005.
- Mitra, A., et al. 2016. Defining planktonic protist functional groups on mechanisms for energy and nutrient acquisition: incorporation of diverse mixotrophic strategies. *Protist* 167:106–120.
- Moeller, H. V., E. Peltomaa, M. D. Johnson, and M. G. Neupert. 2016. Acquired phototrophy stabilises coexistence and shapes intrinsic dynamics of an intraguild predator and its prey. *Ecology Letters* 19:393–402.
- Moore, L. R., A. F. Post, G. Roco, and S. W. Chisholm. 2002. Utilization of different nitrogen sources by the marine cyanobacteria *Prochlorococcus* and *Synechococcus*. *Limnology and Oceanography* 47:989–996.
- Morin, P. 1999. Productivity, intraguild predation, and population dynamics in experimental food webs. *Ecology* 80:752–760.
- Mylus, S. D., K. Klumpers, A. M. de Roos, and L. Persson. 2001. Impact of intraguild predation and stage structure on simple communities along a productivity gradient. *American Naturalist* 158:259–276.
- Not, F., M. Latasa, D. Marie, T. Cariou, D. Vaultot, and N. Simon. 2004. A single species, *Micromonas pusilla* (Prasinophyceae), dominates the eukaryotic picoplankton in the Western English Channel. *Applied and Environmental Microbiology* 70:4064–4072.
- Paine, R. T. 1969. A note on trophic complexity and community stability. *American Naturalist* 103:91–93.
- Passarge, J., S. Hol, M. Escher, and J. Huisman. 2006. Competition for nutrients and light: stable coexistence, alternative stable states, or competitive exclusion? *Ecological Monographs* 76:57–72.
- Polis, G. A., and R. D. Holt. 1992. Intraguild predation: the dynamics of complex trophic interactions. *Trends in Ecology and Evolution* 7:151–154.
- Polis, G. A., C. A. Myers, and R. D. Holt. 1989. The ecology and evolution of intraguild predation: potential competitors that eat each other. *Annual Review of Ecology and Systematics* 20:297–330.
- Price, J. E., and P. J. Morin. 2004. Colonization history determines alternate community states in a food web of intraguild predators. *Ecology* 85:1017–1028.
- Ptácnik, R., U. Sommer, T. Hansen, and V. Martens. 2004. Effects of microzooplankton and mixotrophy in an experimental planktonic food web. *Limnology and Oceanography* 49:1435–1445.
- Ptácnik, R., et al. 2016. A light-induced shortcut in the planktonic microbial loop. *Scientific Reports* 6:29286.
- Raven, J. 1997. Phagotrophy in phototrophs. *Limnology and Oceanography* 42:198–205.
- Rothhaupt, K. O. 1996a. Laboratory experiments with a mixotrophic chrysophyte and obligately phagotrophic and phototrophic competitors. *Ecology* 77:716–724.
- Rothhaupt, K. O. 1996b. Utilization of substitutable carbon and phosphorus sources by the mixotrophic chrysophyte *Ochromonas* sp. *Ecology* 77:706–715.
- Sanders, R. W., and R. J. Gast. 2011. Bacterivory by phototrophic picoplankton and nanoplankton in Arctic waters. *FEMS Microbiology Ecology* 82:242–253.
- Sanders, R. W., K. G. Porter, and D. A. Caron. 1990. Relationship between phototrophy and phagotrophy in the mixotrophic chrysophyte *Poteroiochromonas malhamensis*. *Microbial Ecology* 19:97–109.
- Sanders, R. W., D. A. Caron, J. M. Davidson, M. R. Dennett, and D. M. Moran. 2001. Nutrient acquisition and population growth of a mixotrophic alga in axenic and bacterized cultures. *Microbial Ecology* 42:513–523.
- Skovgaard, A. 1996. Mixotrophy in *Fragilidium subglobosum* (Dinophyceae): growth and grazing responses as functions of light intensity. *Marine Ecology Progress Series* 143:247–253.
- Skovgaard, A., P. J. Hansen, and D. K. Stoecker. 2000. Physiology of the mixotrophic dinoflagellate *Fragilidium subglobosum*. I. Effects of phagotrophy and irradiance on photosynthesis and carbon content. *Marine Ecology Progress Series* 201:129–136.
- Stickney, H. L., R. R. Hood, and D. K. Stoecker. 1999. The impact of mixotrophy on planktonic marine ecosystems. *Ecological Modelling* 125:203–230.
- Stomp, M., J. Huisman, F. de Jongh, A. J. Veraart, D. Gerla, M. Rijkeboer, B. W. Ibelings, U. I. A. Wollenzien, and L. J. Stal. 2004. Adaptive divergence in pigment composition promotes phytoplankton biodiversity. *Nature* 432:104–107.
- Strom, S. L. 2001. Light-aided digestion, grazing and growth in herbivorous protists. *Aquatic Microbial Ecology* 23:253–261.
- Thingstad, T. F., H. Havskum, K. Garde, and B. Riemann. 1996. On the strategy of “eating your competitor”: a mathematical analysis of algal mixotrophy. *Ecology* 77:2108–2118.
- Thompson, P. A., P. J. Harrison, and J. S. Parslow. 1991. Influence of irradiance on cell volume and carbon quota for ten species of marine phytoplankton. *Journal of Phycology* 27:351–360.
- Tilman, D. 1977. Resource competition between plankton algae: an experimental and theoretical approach. *Ecology* 58:338–348.
- Tilman, D. 1990. Constraints and tradeoffs: toward a predictive theory of competition and succession. *Oikos* 58:3–15.
- Tittel, J., V. Bissinger, B. Zippel, U. Gaedke, E. Bell, A. Lorke, and N. Kamjunke. 2003. Mixotrophs combine resource use to outcompete specialists: implications for aquatic food webs. *Proceedings of the National Academy of Sciences of the United States of America* 100:12776–12781.
- Van Baren, M. J., et al. 2016. Evidence-based green algal genomics reveals marine diversity and ancestral characteristics of land plants. *BMC Genomics* 17:267.
- Verity, P. G., C. Y. Robertson, C. R. Tronzo, M. G. Andrews, J. R. Nelson, and M. E. Sieracki. 1992. Relationships between cell volume and the carbon and nitrogen content of marine photosynthetic nanoplankton. *Limnology and Oceanography* 37:1434–1446.
- Ward, B. A., and M. J. Follows. 2016. Marine mixotrophy increases trophic transfer efficiency, mean organism size, and vertical carbon flux. *Proceedings of the National Academy of Sciences of the United States of America* 113:2958–2963.
- Wilken, S., J. Huisman, S. Naus-Wiezer, and E. Van Donk. 2013. Mixotrophic organisms become more heterotrophic with rising temperature. *Ecology Letters* 16:225–233.
- Wilken, S., J. M. H. Verspagen, S. Naus-Wiezer, E. Van Donk, and J. Huisman. 2014a. Biological control of toxic cyanobacteria by mixotrophic predators: an experimental test of intraguild predation theory. *Ecological Applications* 24:1235–1249.
- Wilken, S., J. M. H. Verspagen, S. Naus-Wiezer, E. Van Donk, and J. Huisman. 2014b. Comparison of predator-prey interactions with and without intraguild predation by manipulation of the nitrogen source. *Oikos* 123:423–432.
- Wissinger, S., and J. McGrady. 1993. Intraguild predation and competition between larval dragonflies: direct and indirect effects on shared prey. *Ecology* 74:207–218.
- Worden, A. Z., et al. 2009. Green evolution and dynamic adaptations revealed by genomes of the marine picoeukaryotes *Micromonas*. *Science* 324:268–272.

SUPPORTING INFORMATION

Additional supporting information may be found in the online version of this article at <http://onlinelibrary.wiley.com/doi/10.1002/ey.2874/supinfo>

DATA AVAILABILITY

Model code is available from Zenodo: <https://doi.org/10.5281/zenodo.3350438>